



Mobility of model proteins in hydrogels composed of oppositely charged dextran microspheres studied by protein release and fluorescence recovery after photobleaching

Sophie R. Van Tomme^a, Bruno G. De Geest^b, Kevin Braeckmans^b,
Stefaan C. De Smedt^b, Florence Siepmann^c, Juergen Siepmann^c,
Cornelus F. van Nostrum^a, Wim E. Hennink^{a,*}

^a Department of Pharmaceutics, Utrecht Institute for Pharmaceutical Sciences (UIPS), University Utrecht, P.O. Box 800082, 3508 TB Utrecht, The Netherlands

^b Laboratory of General Biochemistry and Physical Pharmacy, Department of Pharmaceutics, Ghent University, Harelbekestraat 72, 9000 Ghent, Belgium

^c University of Lille, School of Pharmacy, 3, Rue du Professeur Laguesse, 59006 Lille, France

Received 15 June 2005; accepted 12 September 2005

Available online 25 October 2005

Abstract

In this paper, the release of proteins from a novel self-gelling hydrogel based on biodegradable dextran microspheres is investigated. The protein-loaded macroscopic gels are obtained by hydration of mixtures of oppositely charged hydroxyethyl methacrylate-derivatized dextran microspheres with a protein solution. In media of low ionic strength (100 mM Hepes pH 7.0) it was found that the release of the entrapped model proteins (lysozyme, BSA and IgG) was slower than in saline (150 mM NaCl, 100 mM Hepes pH 7.0). The reason behind this observation is that substantial adsorption of the proteins onto the microspheres' surface and/or absorption in the microspheres takes place. Confocal images showed that independent of their crosslink density the microspheres are impermeable for BSA and IgG. BSA, bearing a negative charge at neutral pH, was adsorbed onto the surface of positively charged microspheres. Lysozyme, which is positively charged at neutral pH, was able to penetrate into the negatively charged microspheres. In saline, the gels showed continuous release of the different proteins for 25 to 60 days. Importantly, lysozyme was quantitatively and with full preservation of its enzymatic activity released in about 25 days. This emphasizes the protein friendly technology to prepare the protein-loaded gels. Mathematical modeling revealed that protein release followed Fick's second law, indicating that the systems are primarily diffusion controlled. These results show that these hydrogels are very suitable as injectable matrix for diffusion-controlled delivery of pharmaceutically active proteins. © 2005 Elsevier B.V. All rights reserved.

Keywords: Dextran; Injectable hydrogels; Self-assembling; Mathematical modeling; Diffusion-controlled protein delivery

* Corresponding author. Tel.: +31 30 2536964; fax: +31 30 251 7839.

E-mail address: W.E.Hennink@pharm.uu.nl (W.E. Hennink).

1. Introduction

Hydrogels are an attractive class of materials for the controlled release of pharmaceutical proteins and for tissue engineering applications [1–7]. The release of the entrapped proteins can be tailored by varying the crosslink density, the water content and the polymer composition of the hydrogels. Crosslinking can be established either with chemical or physical methods [8]. The latter is most favorable since the use of organic solvents or crosslinking agents, often toxic and potentially destructive for the protein, is avoided. In physically crosslinked systems non-permanent bonds are created by physical interactions between the polymer chains [9–14]. In recent years there is a growing interest in physically crosslinked systems where gel formation is through self-assembly [15–19]. Network formation can be obtained after mixing the hydrogel components (e.g. stereocomplex gels [20–23]) or after a certain trigger (e.g. temperature [24–28], pH [29,30] or biological stimuli [31]). These systems can be administered by injection as liquid formulation and gelation occurs in situ.

Recently we reported on a novel self-gelling hydrogel based on oppositely charged dextran microspheres [32]. This system combines the injectability of polymeric microspheres with physical crosslinking through ionic interactions. A macroscopic hydrogel is formed by simply mixing aqueous dispersions of anionically and cationically charged microspheres. Importantly, it was demonstrated that the ionic interactions creating the physical network could be broken when exposed to shear. Further, the gel is reformed when the shear is removed, indicating the reversible character of the system. The concept is illustrated in Fig. 1.

This study is focused on the release of proteins in these novel hydrogels, composed of dex-HEMA-MAA and dex-HEMA-DMAEMA microspheres. Dex-HEMA microspheres are degradable at physiological pH and temperature. The network degradation is caused by OH⁻ driven hydrolysis of the carbonate-ester, linking the dextran backbone and the HEMA side chains. The in vitro and in vivo degradability of dex-HEMA microspheres has been reported previously [33–35]. The release of three model proteins varying in isoelectric point (pI) and size was studied as function of the solid content of the gel and the

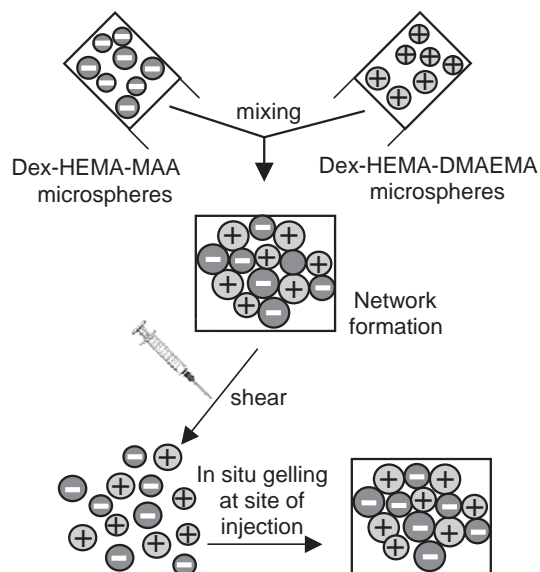


Fig. 1. Schematic presentation of the concept of the in situ gelling system based on oppositely charged dextran microspheres.

crosslink density of the dextran microspheres that form the gel. Possible matrix–protein interactions were studied by adsorption experiments and confocal laser scanning microscopy. Finally, fluorescence recovery after photobleaching was used to gain insight into the mobility of proteins in the complex network of charged polymeric microspheres.

2. Materials and methods

2.1. Materials

Dextran T40 (from *Leuconostoc* ssp.), *N,N,N',N'*-tetramethylethylenediamine (TEMED), 2-hydroxyethyl methacrylate (HEMA) and lysozyme (from hen egg white) were provided by Fluka (Buchs, Switzerland). Poly(ethylene glycol) (PEG) 10,000 and potassium peroxydisulfate (KPS) were purchased from Merck (Darmstadt, Germany). *N*-2-hydroxyethylpiperazine-*N'*-2-ethanesulfonic acid (Hepes) was obtained from Acros Chimica (Geel, Belgium). Methacrylic acid (MAA), dimethylaminoethyl methacrylate (DMAEMA), bovine serum albumin (BSA, fraction V, minimum 96%), fluorescein isothiocyanate bovine serum albumin (FITC-BSA), fluorescein isothiocya-

nate (FITC, isomer I, 90) and *Micrococcus lysodeikticus* were provided by Sigma-Aldrich (Zwijndrecht, The Netherlands). Bovine immunoglobulin G (IgG, fraction II) was obtained from ICN Biomedicals BV (Zoetermeer, The Netherlands). The bicinchoninic acid (BCA) protein assay kit was purchased from Interchim (Montluçon, France). Hydroxyethyl methacrylate-derivatized dextran (dex-HEMA) was synthesized and characterized according to Van Dijk-Wolthuis et al. [36]. Dextran with an M_n of 16,000 Da was selected, ensuring renal excretion during in vivo applications [37]. The DS' (i.e. the number of HEMA groups per 100 glucopyranose units) used in this study were 5, 8 and 18.

2.2. Preparation of charged dex-HEMA microspheres

Negatively and positively charged microspheres were prepared as described previously [32]. In short, the dextran microspheres, with a water content of 70%, were obtained through radical polymerization of dex-HEMA, emulsified in an aqueous poly(ethylene glycol) solution. Addition of either methacrylic acid (MAA) or dimethylaminoethyl methacrylate (DMAEMA) to the polymerization mixture resulted in respectively negatively (dex-HEMA-MAA) and positively (dex-HEMA-DMAEMA) charged microspheres. The crosslinked particles were purified by multiple washing and centrifugation steps and ultimately the microspheres were lyophilized. The particle size and size distribution of the microspheres were determined with a laser blocking technique, using an Accusizer® (model 770, Particle Sizing Systems, Santa Barbara, CA, USA).

The mean volume diameters of the dex-HEMA-MAA and the dex-HEMA-DMAEMA microspheres were 10 μm . The microsphere charge was confirmed by ζ -potential measurements using a Malvern Zetasizer 2000 (Malvern Instruments, Worcestershire, UK) [38]. The ζ -potentials varied from -13 to -16 for dex-HEMA-MAA microspheres and from $+12$ to $+15$ for dex-HEMA-DMAEMA microspheres.

2.3. Formation of physically crosslinked hydrogels using charged microspheres

Hydrogels consisting of equal amounts of positively (dex-HEMA-DMAEMA) and negatively (dex-

HEMA-MAA) charged microspheres were prepared by mixing the lyophilized microspheres. Next, the microsphere mixture was hydrated in Hepes buffer for 1 h (100 mM pH 7.0) at 4 °C. The solid content of the gels was varied between 15% and 30%. Hydrogels containing 1 mg protein per 100 mg gel were prepared by hydration of the microsphere mixture in a protein solution (25 mg/mL) in 100 mM Hepes (100 mM pH 7.0).

2.4. Adsorption and absorption of proteins to the microspheres

Possible absorption and adsorption of proteins to the negatively or positively charged microspheres were studied by incubating 10 mg dry microspheres with 1 mL of protein solution 500 $\mu\text{g}/\text{ml}$ in Hepes buffer (100 mM, pH 7.0). After 1 h of incubation at room temperature the dispersions were centrifuged (1 min 10,000 rpm) and the protein concentration in the supernatant was determined with the BCA® Protein Assay (described in Section 2.7). Subsequently, the microsphere pellet was redispersed in 1 ml 150 mM NaCl, Hepes buffer pH 7.0 and incubated for 1 day at room temperature. Thereafter, the dispersions were treated and analyzed as described above.

Confocal images of FITC-labeled lysozyme and BSA in the gels were taken using a confocal scanning laser microscope (model MRC1024 UV, Bio-Rad, Hemel Hempstead, UK).

2.5. Rheological experiments

Rheological experiments were performed on hydrogels (25% solid) with and without protein loading. The rheological measurements on the hydrogels were performed using a controlled stress rheometer (AR1000-N, TA Instruments, Etten-Leur, The Netherlands), equipped with an acrylic flat plate geometry (20 mm diameter) and a gap of 500 μm [32]. Hydrogels were prepared as described in Section 2.3 and thereupon introduced between the two plates. A solvent trap was used to prevent evaporation of the solvent. The viscoelastic properties of the gels were determined by measuring the G' (shear storage modulus) and G'' (loss modulus) at 20 °C with a constant strain of 1% and constant frequency of 1 Hz. Creep experiments were done to evaluate the extent of

recovery of the material after deformation. Therefore a shear stress of 50 Pa was applied while the strain was monitored. After 5 min the stress was removed and the recovery of the sample was monitored by measuring the strain during 10 min.

2.6. In vitro protein release

Hydrogels were prepared and loaded with the various proteins as described in Section 2.3. Lysozyme (Mw 14,000 g/mol), BSA (Mw 67,000 g/mol) and IgG (Mw 150,000 g/mol) were used as model proteins. Their diffusion coefficients in water (D_0) are respectively: 1.04×10^{-6} cm²/s [39], 0.59×10^{-6} cm²/s [39] and 0.40×10^{-6} cm²/s [40]. The hydrodynamic diameter of the proteins (d) was calculated using the Einstein–Stokes Eq. (1):

$$D_0 = \frac{kT}{3\pi\eta d} \quad (1)$$

where D_0 is the diffusion coefficient of the protein, k is the Boltzmann constant, T is the absolute temperature and η is the viscosity of the solvent. The calculated hydrodynamic diameters for lysozyme, BSA and IgG are respectively 4.1, 7.2 and 10.7 nm.

Different protein-loaded hydrogels were prepared, altering the solid content of the gels (15%–30%) and the DS of the microspheres (DS 5, 8, 18). Each formulation was made in duplo. Non-protein loaded hydrogels were also included in the study. For every formulation, 500 mg gel was prepared in 2 mL eppendorf cups that were weighed in advance. After hydration the gels were transferred into the release device (described below), closed with a rubber stop and the empty eppendorf cups were weighed again to determine the exact weight of the gel introduced in the device. The release device is made of polyoxymethylene and consists of a gel and a release compartment, with a diameter of respectively 8.5 and 15 mm and length of 8.8 and 30 mm (Fig. 2). As a result, cylind-

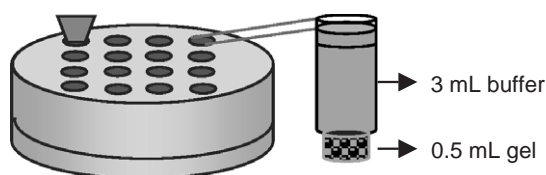


Fig. 2. Schematic presentation of the release device.

rical gels of 8.5 × 8.8 mm (diameter × length) were obtained. Release buffer (3 mL, 100 mM Hepes pH 7.0, 0.02% NaN₃, with and without 150 mM NaCl) was added to each formulation and the device was incubated on a shaking plate at 37 °C. Samples of 0.5 mL were taken at regular time intervals and replaced by an equal volume of fresh buffer. The release samples were analyzed for their protein concentration using the BCA[®] Protein assay described in the next section.

2.7. Determination of protein concentration and enzymatic activity of lysozyme in release samples

The protein concentration in the release samples was determined with the BCA[®] Protein Assay [41]. Standard protein solutions (concentration range 0.010–1 mg/mL) were prepared to generate calibration curves. Release samples (25 μL) were pipetted into a 96-micro-wells plate and 200 μL of working reagent (=BCA reagent A: BCA reagent B, 50:1 v/v) was added. The plates were incubated for 30 min at 37 °C followed by cooling down to room temperature. Subsequently the absorbance was measured at 550 nm with a Microplate Manager[®] (Bio-Rad Laboratories, Hercules, CA, USA).

The enzymatic activity of lysozyme in some selected release samples was determined. The assay is based on the hydrolysis of the outer cell membrane of *M. lysodeikticus*, resulting in solubilization of the affected bacteria and consequent decrease of light scattering [42]. The release samples were diluted to a concentration of 50–100 μg/mL. Next, 10 μL of sample was added to 1.3 mL of *M. lysodeikticus* suspension (0.2 mg/mL, 100 mM Hepes buffer pH 7.0) and the decrease in turbidity was measured for 3 min at 450 nm. The percent remaining enzyme activity was obtained by comparing the activity to that of a reference lysozyme solution (100 μg/mL).

UV scans (Perkin-Elmer Lambda 2 UV/VIS spectrophotometer, Überlingen, Germany, 250–350 nm) of release samples containing lysozyme were taken and compared to a scan of a reference lysozyme solution (100 μg/mL) to verify the possible presence of protein aggregates. Lysozyme denaturation was checked by fluorescence spectroscopy of release samples (Fluorolog fluorimeter, Jobin Yvon Horriba, 300–450 nm) and also compared to a freshly made lysozyme solution (23 μg/mL).

2.8. Mathematical modeling of *in vitro* protein release

An analytical solution of Fick's second law of diffusion was used to quantitatively describe protein release from the investigated hydrogels. The hydrogels are regarded as monolithic structures since the proteins were molecularly dispersed in the macroscopic gels. Furthermore, the model considers that the edges of the cylindrical gels were not exposed to the release medium. Thus, the mathematical analysis could be restricted to one dimension and the release kinetics could be described as follows [43]:

$$\frac{\partial c}{\partial t} = D \cdot \frac{\partial^2 c}{\partial x^2} \quad (2)$$

where c denotes the concentration of the protein within the polymeric system, being a function of time t and position x ; D represents the apparent diffusion coefficient of the protein.

Considering perfect sink conditions throughout the experiment and the fact that only one circular surface of the cylindrical gels was exposed to the release medium, the following solution of Fick's second law of diffusion can be derived and used to describe protein release from the investigated hydrogels [43]:

$$\frac{M_t}{M_\infty} = 1 - \sum_{n=0}^{\infty} \frac{8}{(2 \cdot n + 1)^2 \cdot \pi^2} \cdot \exp\left(-\frac{(2 \cdot n + 1)^2 \cdot \pi^2}{4 \cdot L^2} \cdot D \cdot t\right) \quad (3)$$

where M_t and M_∞ , represent the absolute cumulative amounts of protein released at time t , and infinite time, respectively; L denotes the height of the cylindrical hydrogel.

If protein release leveled off below 100%, the experimentally determined plateau value (amount of mobile protein) was considered as 100% reference value for protein diffusion.

2.9. Fluorescence recovery after photobleaching (FRAP)

FRAP was used to study the mobility of the proteins in the gels composed of oppositely charged particles, as well as in the microspheres themselves [44].

The FRAP measurements were performed using a setup as described previously [45,46]. In detail, a confocal scanning laser microscope (model MRC1024 UV, Bio-Rad, Hemel Hempstead, UK) modified for bleaching arbitrary regions, was used. The 488-nm line of a 4 W Ar-ion laser (model Stabilite 2017; Spectra-Physics, Darmstadt, Germany) was used to bleach uniform disks with a typical diameter of 25 μm . It is assumed that the bleaching phase is very short (100 to 200 ms) so that the amount of fluorescence recovery that will take place during bleaching is negligible compared to the characteristic recovery time. The microscope was equipped with a 10 \times objective lens (CFI Plan Apochromat; Nikon, Badhoevedorp, The Netherlands). Next, a highly attenuated laser beam measured the fluorescence recovery in the bleached area, which is due to the diffusion of fluorescent probes from the surrounding unbleached area into the bleached spot. The diffusion coefficient can be calculated from the experimental recovery curve by fitting of the appropriate FRAP model. The derivation of the FRAP model for a uniform disk bleached by a low numerical aperture lens has been described earlier [47].

The gels were loaded with fluorescein isothiocyanate (FITC) labeled proteins. FITC-BSA was used as provided by the supplier whereas lysozyme was labeled as follows: 300 mg lysozyme and 12 mg FITC were each dissolved in 60 mL borate buffer (100 mM, pH 8.5). While stirring, the FITC solution was added drop wise to the lysozyme solution and the resulting solution was stirred for 16 h. Next, the protein solution was extensively dialyzed against water (at 4 $^\circ\text{C}$) and the FITC-lysozyme was collected after freeze-drying.

Protein stock solutions were prepared by dissolving 180 mg lysozyme or BSA and 20 mg FITC-lysozyme, respectively, FITC-BSA in 10 mL buffer (Hepes 100 mM pH 7.0).

The microspheres were prepared as described in Section 2.2. After the washing and centrifugation steps, 500 mg of both dex-HEMA-MAA and dex-HEMA-DMAEMA microspheres were dispersed in 5 mL buffer (Hepes 100 mM pH 7) and subsequently vigorously mixed. The vials were rinsed with 5 mL buffer that was subsequently added to the particle dispersion. After centrifugation (5 min 2000 rpm) 200 mg gel was transferred into eppendorf vials (1.5

mL) and 100 μ L fluorescently labeled protein stock solution was added. These mixtures were again intensively vortexed and centrifuged (5 min 2000 rpm). Samples containing either positively or negatively charged microspheres were prepared in the same way. Just after preparation, the supernatant in the vials containing protein-loaded gels composed of oppositely charged microspheres was colorless and the gels were yellow, whereas in the vials containing only microspheres of the same charge, the supernatant had a bright yellow color. This indicates that the fluorescently labeled protein was fully entrapped in the physically crosslinked network.

To perform FRAP experiments a spatula tip of the protein-loaded hydrogel was placed on an objective glass, on which an adhesive spacer (Secure-Seal Spacer, Molecular Probes, Leiden, The Netherlands) of 0.5 mm thickness (adhering at both sides) was fixed, and subsequently protected with a cover glass. In this way evaporation and convection in the sample were prevented.

As a control, the diffusion coefficients of the fluorescent probes were measured in a sucrose solution (50% w/w). The viscosity of the sucrose–protein solutions was determined using a Lauda MGW 540 SK viscosimeter (Lauda MGW, Germany).

3. Results and discussion

3.1. Adsorption and absorption of proteins to the microspheres

Confocal images were taken to visualize the distribution of the proteins in the gel matrices. Fig. 3A and B show respectively lysozyme and BSA in gels composed of dextran microspheres with DS 5 in a medium with low ionic strength (100 mM Hepes, pH 7.0, ionic strength 27 mM). This figure illustrates that lysozyme was able to penetrate into the microspheres, while BSA was only visible between the microspheres. The same results (not shown) were found for the gels composed of microspheres with higher crosslink densities (DS 8 and 18), indicating that lysozyme ($d_h=4.1$ nm) is small enough to diffuse into the microspheres even when the DS is 18, while BSA ($d_h=7.2$ nm) is too large to penetrate into the microspheres. Fig. 3A also shows that lyso-

zyme is not able to penetrate into all microspheres. Control experiments (Fig. 3C and D) reveal that lysozyme is able to penetrate into negatively charged microspheres, whereas positively charged microspheres do not absorb this protein. This result can be explained by the positive charge that lysozyme bears at neutral pH ($pI_{\text{lysozyme}}=9.3$ [48]). BSA, which is negatively charged at pH 7 ($pI_{\text{BSA}}=4.7$ [49]), is adsorbed onto the surface of positively charged microspheres (Fig. 3B). No penetration into neither the negatively nor positively charged microspheres is observed. Adsorption and/or absorption of the proteins to the microspheres were quantified as described in Section 2.4. Table 1 lists the results. In the presence of negatively charged microspheres, the microspheres ad(b)sorbed 75% of the added lysozyme in medium of low ionic strength (100 mM Hepes, pH 7.0), whereas no adsorption onto the positive microspheres was found. BSA adsorbed onto positively charged microspheres (35% of amount added) and showed no adsorption onto negatively charged particles. These results are in good agreement with the confocal images and can be explained by the net charge that BSA and lysozyme have at neutral pH. When the protein solutions were added to mixtures of positively and negatively charged microspheres, the adsorbed amount was considerably lower (50% and 20% for lysozyme and BSA, respectively), indicating that the proteins are only able to interact with part of the microsphere population. IgG (polyclonal, pI 5–10) showed the least adsorption to the particles (5%–20%), independent of the charge of the microspheres. When the microspheres, preadsorbed with protein, were incubated in Hepes buffered saline (150 mM NaCl, 100 mM Hepes, pH 7.0) almost quantitative desorption occurred, again indicating that the adsorption is due to electrostatic interactions between the proteins and microspheres of opposite charge.

3.2. In vitro protein release

To study the in vitro protein release from the ionically crosslinked gels, three model proteins, lysozyme, BSA and IgG, differing in hydrodynamic radius, molecular weight and isoelectric point were used. The influence of protein properties, solid content of the gels, DS of the microspheres and the ionic strength of the release buffer was investigated.

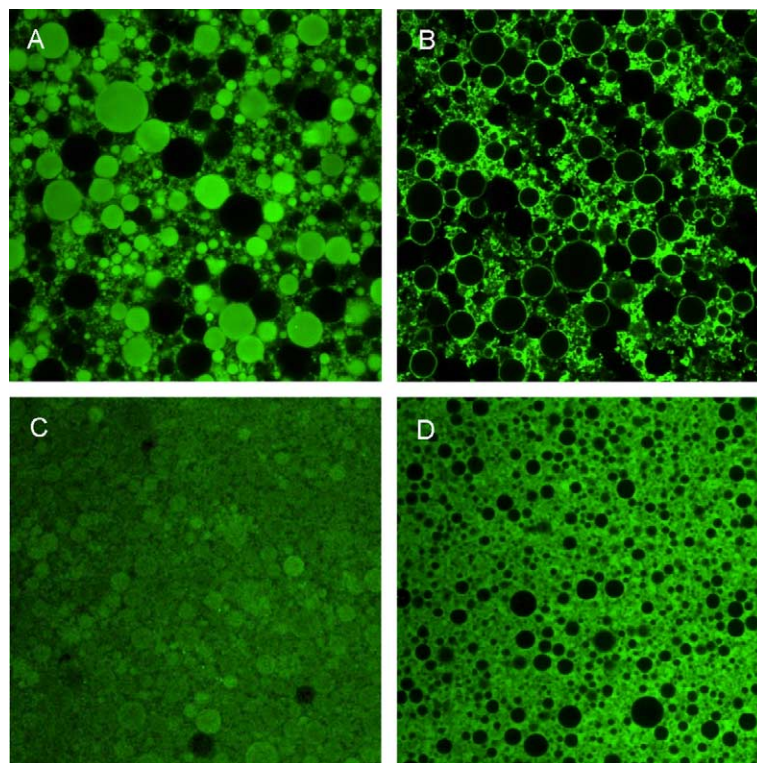


Fig. 3. Confocal images of FITC-lysozyme (A) and FITC-BSA (B) entrapped in hydrogels prepared by mixing oppositely charged dextran microspheres (DS 5). C and D show the confocal images of FITC-lysozyme in dispersions of negatively and positively charged dextran microspheres.

Since the proteins investigated bear a charge at neutral pH and show adsorption onto the microspheres, it cannot be excluded that by this process the interaction between the microspheres is dimin-

ished. It was shown that the rheological parameters (G' , G'' , $\tan(\delta)$) and the recovery during creep of a protein-loaded and control gel prepared in HEPES buffer (100 mM, pH 7.0) were equal, indicating that proteins do not influence the network properties of the gel.

A continuous release of the proteins from both the 15% and 30% gels composed of microspheres with DS 5, 8 and 18 was observed in HEPES buffered saline (100 mM, pH 7.0, 150 mM NaCl). Fig. 4 shows a representative example. This figure illustrates that 50% of the entrapped lysozyme, BSA and IgG was released in 4, 5 and 60 days, respectively.

The structure of proteins might be changed after their release from polymeric matrices because of stress factors applied during the preparation of the protein-loaded materials [50]. Also, degradation of the matrices might be associated with protein degradation [51–55]. Therefore, we studied the structure of the released lysozyme with spectroscopic techniques

Table 1
Influence of ionic strength and protein charge on the adsorption and/or absorption of lysozyme, BSA and IgG to charged microspheres

Protein (charge)	Microsphere charge	% adsorbed/absorbed after 1 h without NaCl	% adsorbed/absorbed after 1 day of NaCl after 1 h
Lysozyme (+)	–	75	0
	+	0	0
	+ and –	50	0
BSA (–)	–	0	0
	+	35	10
	+ and –	20	10
IgG (polyclonal)	–	5	0
	+	10	5
	+ and –	20	5

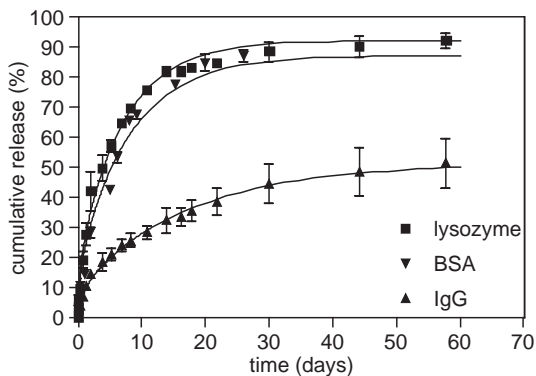


Fig. 4. Cumulative release of lysozyme (■), BSA (▼) and IgG (▲) from hydrogels (15% solid, DS 8). Symbols: experimental values; curves: fitted theory (Eq. (3)). Data are shown as average ($n=2$).

(fluorescence, UV) and a bioactivity assay was done to quantify its enzymatic activity. Fluorescence spectroscopy revealed that there were no shifts in the maximum fluorescence intensity peak of the released protein when compared to native lysozyme, indicating that no structural damage of the protein has occurred. Moreover, UV scans showed no shift in maximum absorbance and no extra peaks in the 310–350 nm region, which indicates that no protein aggregates were formed. Finally, the lysozyme activity assay showed that the specific activity of released lysozyme was the same as that of native lysozyme. It can therefore be concluded that neither degradation nor aggregation of the lysozyme during preparation of the gel and/or during release had occurred.

Good agreement between the experimentally measured and theoretically calculated (Eq. (3)) protein release kinetics was obtained in all cases (e.g. Figs. 4 and 5). This indicates that the release of the model proteins from the hydrogels is primarily diffusion controlled during the entire release period. Dependent on their size and surface charge, all proteins, are hindered by the microsphere network. Smaller proteins with a hydrodynamic diameter smaller than the pores in the dextran microspheres are able to diffuse in and out of the microspheres. In contrast, larger protein molecules are not able to penetrate into the microspheres and have to search their way between the microspheres, leading to a longer journey before they reach the gel surface and diffuse into the release medium. But for both extreme situations, and in agreement with observations, the release of both

small and large proteins is governed by diffusion (Fig. 4; Table 2). Based on the mathematical analysis, the apparent diffusion coefficients of the respective proteins in the gels was determined (Table 2). The observed differences correlate very well with the molecular weight and hydrodynamic radii of the proteins ($D_{(\text{lysozyme})} > D_{(\text{BSA})} > D_{(\text{IgG})}$). In all cases, except for lysozyme with microspheres of DS 8 and 18 and IgG with microspheres of DS 18, doubling the percent solid content did not lead to a significant decrease in D (Unpaired t test, $p > 0.05$). The insignificant differences between the diffusion coefficients of the proteins in the gels of 15% and 30% solid content can be explained as follows. In the initial situation, 30% gels will be composed of 30% dry microspheres hydrated with 70% water (the microspheres were prepared as such that their equilibrium water content amounted 70%), leaving no water in the spaces between the microspheres. In 15% gels, obtained by mixing 150 mg dry dextran microspheres with 850 mg water, the dry microspheres will absorb 350 mg water, meaning 500 mg (50% of the total hydrogel mass) is present between the microspheres. During the release experiment the gels are brought into contact with an excess of water, which makes that they swell. A higher percent of microspheres results in a higher swelling ratio (1.3 for 15%; 1.8 for 30%) of the macroscopic gel, eventually leading to gels of about the same

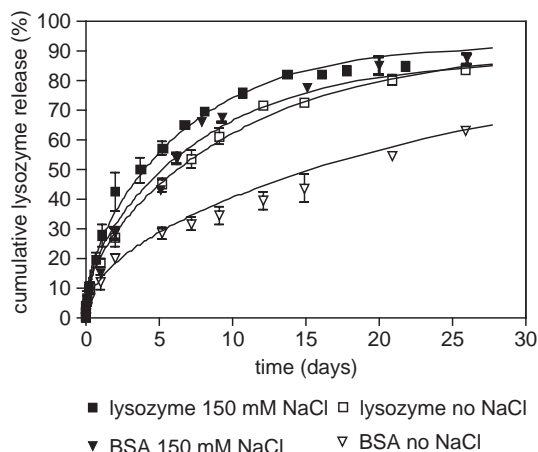


Fig. 5. The release of lysozyme (■) and BSA (▼) from a 15% gel (DS 8) in 100 mM Hepes, 150 mM NaCl, pH 7.0, 0.02% NaN_3 (full symbols) and 100 mM Hepes, pH 7.0, 0.02% NaN_3 (open symbols). Symbols: experimental values; curves: fitted theory (Eq. (3)). Data are shown as average ($n=2$).

Table 2
Diffusion coefficients of lysozyme, BSA and IgG determined by fitting Eq. (3) to the experimentally measured protein release kinetics: effects of the solid content of the hydrogel, type of protein, degree of substitution of dextran

Solid content	Protein	DS	D , 10^{-7} cm ² /s (\pm S.D.)	R^2
15%	Lysozyme	5	5.4 ± 0.6	0.99–1.00
		8	5.1 ± 0.1	0.99–1.00
		8 ^a	3.4 ± 0.3	0.99–1.00
	BSA	18	8.8 ± 0.1	0.98–0.99
		5	4.3 ± 0.2	0.98–0.99
		8	4.4 ± 0.0	0.99
	IgG	8 ^a	1.5 ± 0.1	0.97–0.99
		18	6.8 ± 0.8	0.99
		5	2.1 ± 0.1	0.99
30%	Lysozyme	8	2.1 ± 0.2	1.00
		18	3.6 ± 0.1	0.99
		5	4.1 ± 0.6	0.99–1.00
	BSA	8	3.9 ± 0.2	0.99
		18	3.7 ± 0.0	1.00
		5	4.1 ± 0.2	0.97–0.98
	IgG	8	4.1 ± 0.5	0.97
		18	5.0 ± 0.2	0.98
		5	2.1 ± 0.5	0.98–0.99
		8	2.6 ± 0.2	0.99–1.00
		18	2.4 ± 0.3	0.99

Unless indicated otherwise, the release medium was Hepes buffer (100 mM, pH 7.0, 0.02 % NaN₃, 150 mM NaCl).

^a Release medium: Hepes buffer (100 mM, pH 7.0, 0.02 % NaN₃).

equilibrium water content (85%–90%). The data given in Table 2 also show that the 15% hydrogels composed of microspheres of DS 18 (highest crosslink density) exhibited the fastest release. We have previously shown that dextran gels with DS above 10 are dimensionally stable [56]. It can be expected that due to swelling the microspheres with a low DS (5 and 8) are pressed onto each other, which will restrict diffusion of the protein. However, the high crosslink density (DS 18) prevents strong swelling of the microspheres, leading to larger pores between the microspheres when compared to the other gels and resulting in the faster release.

Table 2 shows that the diffusion coefficients of the different model proteins in the 30% gels are not dependent on the microsphere crosslink densities. Confocal images (Fig. 3A) showed that lysozyme is absorbed by negatively charged microspheres, independent of their crosslink density. As a result, lysozyme is distributed in and between the microspheres.

Hence, the lysozyme release is not influenced by the crosslink density of the microspheres and will be comparable for DS 5, 8 and 18. Confocal images (Fig. 3B) also showed that BSA is unable to penetrate into the microspheres, independent of their crosslink density. Consequently, BSA is only present in the pores between the microspheres resulting in a release rate that is independent of the DS of the microspheres.

The release of lysozyme and BSA release from 15% gels composed of microspheres with DS 8 was studied in media of low (100 mM Hepes, pH 7.0) and physiological ionic strength (100 mM Hepes, pH 7.0, 150 mM NaCl) (Fig. 5.). Eq. (3) was fitted to the experimentally determined protein release kinetics and the calculated diffusion coefficients are reported in Table 2. In media with physiological ionic strength, the diffusion coefficients of lysozyme and BSA were, respectively, 1.5 and 3 times higher than in media with low ionic strength. In both media full release was observed, indicating that the adsorption/absorption, occurring in media of low ionic strength, is reversible. Adsorption/absorption and subsequent desorption processes retard the mobility of the proteins in the gels and will consequently lower their diffusion coefficients in media of low ionic strength.

3.3. Fluorescence recovery after photobleaching (FRAP)

To study the mobility of lysozyme and BSA on a micro scale in the microsphere dispersions and gels, FRAP measurements were performed. As a control,

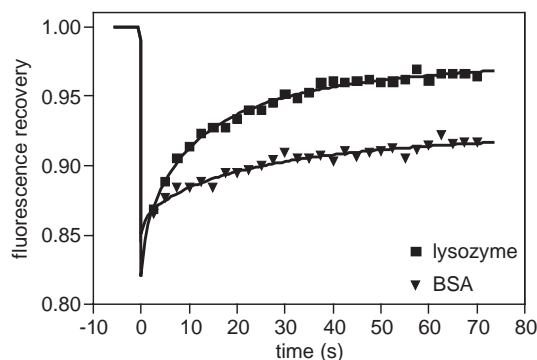


Fig. 6. Fluorescence recovery after photobleaching of FITC-lysozyme (■) and FITC-BSA (▼) in dex-HEMA-MAA/dex-HEMA-DMAEMA hydrogels in Hepes buffer (100 mM, pH 7.0, 150 mM NaCl).

Table 3
Diffusion coefficients (10^{-8} cm²/s) of the model proteins in gels (30% solid) determined with FRAP (data are shown as averages \pm standard deviation ($n=5-7$))

Gels	DS			
	5	8	8 ^a	18
Lysozyme	6.9 \pm 0.8	7.2 \pm 1.0	14 \pm 2.0	3.8 \pm 1.2
BSA	3.1 \pm 0.6	2.2 \pm 0.6	8.5 \pm 3.0	0.8 \pm 0.2
Dispersions (DS 8)	Negatively charged microspheres		Positively charged microspheres	
Lysozyme	4.6 \pm 1.2		31 \pm 2	
BSA	82 \pm 16		4.0 \pm 1.0	

Unless indicated otherwise, the medium was Hepes buffer (100 mM, pH 7.0, 0.02% NaN₃).

^a Hepes buffer (100 mM, pH 7.0, 0.02% NaN₃, 150 mM NaCl).

the diffusion coefficients of the proteins were determined in 50% sucrose solutions. This resulted in diffusion coefficients in water of 0.85×10^{-6} cm²/s (lysozyme) and 0.31×10^{-6} cm²/s (BSA). Fig. 6 shows some representative bleaching and recovery curves. The diffusion coefficients of the proteins in gels composed of microspheres with DS 5, 8 and 18 and dispersions of either cationically or anionically charged microspheres with DS 8, as determined by FRAP, are listed in Table 3. Lysozyme and BSA present in dispersions (100 mM Hepes, pH 7.0) containing non-interacting positively charged or negatively charged microspheres, respectively, have diffusion coefficients similar to those in water. Obviously, the proteins are repelled by the equal charges of the microspheres and diffuse freely through the dispersions. Upon mixing of the positively charged lysozyme with interacting negatively charged microspheres or negatively charged BSA with positively charged microspheres, the opposite phenomenon occurs. The proteins are ionically attracted to the spheres, resulting in 10–20 times lower diffusion coefficients as compared to their values in water. Diffusion coefficients of both proteins in gels composed of equal amounts of positively and negatively charged microspheres (100 mM Hepes, pH 7.0) were about the same as those observed in microsphere dispersions having opposite charge as the proteins. To minimize the ionic interactions between the proteins and the microspheres, FRAP was performed on gels (DS 8) containing 150 mM NaCl protein solution

(Table 3). In these hydrogels, the diffusion of lysozyme and BSA was, respectively, 2 to 4 times faster than in low ionic strength media. These findings are in good agreement with the adsorption and protein release data as described in Sections 3.1 and 3.2. In general, the diffusion coefficients obtained with FRAP are 5 to 20 times smaller than the D 's calculated from the release experiments. These discrepancies result from the differences in experimental setup. The diffusion coefficients of the proteins during their release are macroscopic D 's, whereas those measured with FRAP are on a microscopic level. It might be possible that in gels two populations of protein molecules are present. One with a high mobility, present in the pores between the microspheres and a diffusion coefficient (almost equal) as that in water, and one fraction with restricted mobility (adsorbed by the microspheres). The fraction of protein molecules with high mobility diffuses too rapidly for our confocal microscope to determine their D and consequently the D of the protein molecules interacting with the microspheres is obtained using FRAP.

4. Conclusions

Physically crosslinked hydrogels are an attractive class of protein delivery systems since, during preparation and protein loading, harsh crosslinking conditions are avoided, thereby maintaining the biological activity of the proteins. This paper reports on the in vitro protein release from an injectable self-assembling hydrogel based on oppositely charged dextran microspheres. The gels show a continuous release of the entrapped model proteins with full preservation of the enzymatic activity of lysozyme. This emphasizes the protein-friendly nature of the hydrogel. In conclusion, these hydrogel systems are very suitable for the diffusion-controlled release of pharmaceutical proteins. At present we are studying the degradation behavior of the gels and the in vivo protein release.

References

- [1] A.S. Hoffman, Hydrogels for biomedical applications, Adv. Drug Deliv. Rev. 43 (2002) 3–12.
- [2] K.Y. Lee, D.J. Mooney, Hydrogels for tissue engineering, Chem. Rev. 101 (2001) 1869–1880.

- [3] J.L. Drury, D.J. Mooney, Hydrogels for tissue engineering: scaffold design variables and applications, *Biomaterials* 24 (2003) 4337–4351.
- [4] N.A. Peppas, P. Bures, W. Leobandung, H. Ichikawa, Hydrogels in pharmaceutical formulations, *Eur. J. Pharm. Biopharm.* 50 (2000) 27–46.
- [5] J. Panyam, V. Labhasetwar, Biodegradable nanoparticles for drug and gene delivery to cells and tissue, *Adv. Drug Deliv. Rev.* 55 (3) (2002) 329–347.
- [6] S. Freiberg, X.X. Zhu, Polymer microspheres for controlled drug release, *Int. J. Pharm.* 282 (2004) 1–18.
- [7] V.R. Sinha, A. Trehan, Biodegradable microspheres for protein delivery, *J. Control. Release* 90 (2003) 261–280.
- [8] W.E. Hennink, C.F. van Nostrum, Novel crosslinking methods to design hydrogels, *Adv. Drug Deliv. Rev.* 54 (2002) 13–36.
- [9] S. Nagahara, T. Matsuda, Hydrogel formation via hybridization of oligonucleotides derivatized in water-soluble vinyl polymers, *Polym. Gels Netw.* 4 (1996) 111–127.
- [10] R.J.H. Stenekes, H. Talsma, W.E. Hennink, Formation of dextran hydrogels by crystallization, *Biomaterials* 22 (2001) 1891–1898.
- [11] P. Gacesa, Alginates, *Carbohydr. Polym.* 8 (1988) 161–182.
- [12] W.R. Gombotz, S.F. Wee, Protein release from alginate matrices, *Adv. Drug Deliv. Rev.* 31 (1998) 267–285.
- [13] J.A. Rowley, G. Madlambayan, D.J. Mooney, Alginate hydrogels as synthetic extracellular materials, *Biomaterials* 20 (1999) 45–53.
- [14] J. Berger, M. Reist, J.M. Mayer, O. Felt, N.A. Peppas, R. Gurny, Structure and interactions in covalently and ionically crosslinked chitosan hydrogels for biomedical applications, *Eur. J. Pharm. Biopharm.* 57 (2004) 19–34.
- [15] N. Sreenivasachary, J.M. Lehn, Gelation-driven component selection in the generation of constitutional dynamic hydrogels based on guanine-quartet formation, *Proc. Natl. Acad. Sci. U. S. A.* 102 (17) (2005) 5938–5943.
- [16] I.W. Hamley, I.A. Ansari, V. Castelletto, H. Nuhn, A. Rosler, H.A. Klok, Solution self-assembly of hybrid block copolymers containing poly(ethylene glycol) and amphiphilic β -strand peptide sequences, *Biomacromolecules* 6 (3) (2005) 1310–1315.
- [17] K.S. Anseth, A.T. Metters, S.J. Bryant, P.J. Martens, J.H. Elisseeff, C.N. Bowman, In situ forming degradable networks and their application in tissue engineering and drug delivery, *J. Control. Release* 78 (2002) 199–209.
- [18] B. Balakrishnan, A. Jayakrishnan, Self-cross-linking biopolymers as injectable in situ forming biodegradable scaffolds, *Biomaterials* 26 (2005) 3941–3951.
- [19] G. Tae, J.A. Kornfield, J.A. Hubbell, Sustained release of human growth hormone from in situ forming hydrogel using self-assembly of fluoroalkyl-ended poly(ethylene glycol), *Biomaterials* 26 (2005) 5259–5266.
- [20] S.J. de Jong, S.C. de Smedt, M.W.C. Wahls, J. Demeester, J.J. Kettenes-van den Bosch, W.E. Hennink, Novel self-assembled hydrogels by stereocomplex formation in aqueous solution of enantiomeric lactic acid oligomers grafted to dextran, *Macromolecules* 33 (2000) 3680–3686.
- [21] S.J. de Jong, B. Van Eerdenbrugh, C.F. van Nostrum, J.J. Kettenes-van den Bosch, W.E. Hennink, Physically cross-linked dextran hydrogels by stereocomplex formation of lactic acid oligomers: degradation and protein release behavior, *J. Control. Release* 71 (2001) 261–275.
- [22] G.W. Bos, J.J.L. Jacobs, J.W. Koten, S. VanTomme, T. Veldhuis, C.F. van Nostrum, W. Den Otter, W.E. Hennink, In situ crosslinked biodegradable hydrogels loaded with IL-2 are effective tools for local IL-2 therapy, *Eur. J. Pharm. Sci.* 21 (2004) 561–567.
- [23] S.M. Li, M. Vert, Synthesis, characterization and stereocomplex-induced gelation of block copolymers prepared by ring opening polymerization of L(D)-lactide in the presence of poly(ethylene glycol), *Macromolecules* 36 (2003) 8008–8014.
- [24] E. Ruel-Gariepy, J.C. Leroux, In situ-forming hydrogels—review of temperature-sensitive systems, *Eur. J. Pharm. Biopharm.* 58 (2) (2004) 409–426.
- [25] B. Jeong, S.W. Kim, Y.H. Bae, Thermosensitive sol–gel reversible hydrogels, *Adv. Drug Deliv. Rev.* 54 (2002) 37–51.
- [26] X. Huang, T.L. Lowe, Biodegradable thermoresponsive hydrogels for aqueous encapsulation and controlled release of hydrophilic model drugs, *Biomacromolecules* 6 (4) (2005) 2131–2139.
- [27] D. Cohn, A. Sosnik, S. Garty, Smart hydrogels for in situ generated implants, *Biomacromolecules* 6 (2005) 1168–1175.
- [28] D.J. Pochan, J.P. Schneider, J. Kretsinger, B. Ozbas, K. Rajagopal, L. Haines, Thermally reversible hydrogels via intramolecular folding and consequent self-assembly of a de novo designed peptide, *J. Am. Chem. Soc.* 125 (2003) 11802–11803.
- [29] R. Zhang, M. Tang, A. Bowyer, R. Eisenthal, J. Hubble, A novel pH- and ionic-strength-sensitive carboxy methyl dextran hydrogel, *Biomaterials* 26 (22) (2005) 4677–4683.
- [30] H.C. Chiu, Y.F. Lin, Y.H. Hsu, Effects of acrylic acid on preparation and swelling properties of pH-sensitive dextran hydrogels, *Biomaterials* 23 (4) (2002) 1103–1112.
- [31] Y. Murakami, M. Maeda, Hybrid hydrogels to which single-stranded (ss) DNA probe is incorporated can recognize specific ssDNA, *Macromolecules* 38 (2005) 1535–1537.
- [32] S.R. Van Tomme, M.J. van Steenberg, S.C. De Smedt, C.F. van Nostrum, W.E. Hennink, Self-gelling hydrogels based on oppositely charged dextran microspheres, *Biomaterials* 26 (14) (2005) 2129–2135.
- [33] W.N.E. van Dijk-Wolthuis, M.J. van Steenberg, W.J.M. Underberg, W.E. Hennink, Degradation kinetics of methacrylated dextrans in aqueous solution, *J. Pharm. Sci.* 86 (4) (1997) 413–417.
- [34] O. Franssen, L. Vandervennet, P. Roders, W.E. Hennink, Degradable dextran hydrogels: controlled release of a model protein from cylinders and microspheres, *J. Control. Release* 60 (1999) 211–221.
- [35] J.A. Cadée, L.A. Brouwer, W. den Otter, W.E. Hennink, M.J.A. van Luyn, A comparative biocompatibility study of microspheres based on crosslinked dextran or poly(lactic-co-glycolic)acid after subcutaneous injection in rats, *J. Biomed. Mater. Res.* 56 (4) (2001) 600–609.
- [36] W.N.E. van Dijk-Wolthuis, S.K.Y. Tsang, J.J. Kettenes-van Bosch, W.E. Hennink, A new class of polymerizable dextrans

- with hydrolyzable groups: hydroxyethyl methacrylated dextran with and without oligolactate spacer, *Polymer* 38 (1997) 6235–6242.
- [37] G. Arturson, G. Wallenius, The renal clearance of dextran of different molecular sizes in normal humans, *Scand. J. Clin. Lab. Invest.* 1 (1964) 81–86.
- [38] B.G. De Geest, C. Déjugnat, G.B. Sukhorukov, K. Braeckmans, S.C. De Smedt, J. Demeester, Self-rupturing microcapsules, *Adv. Mater.* 17 (2005) 2357–2361.
- [39] E.W. Merrill, K.A. Dennison, C. Sung, Partitioning and diffusion of solutes in hydrogels of poly(ethylene oxide), *Biomaterials* 14 (1993) 1117–1126.
- [40] K. Burczak, T. Fujisato, M. Hatada, Y. Ikada, Protein permeation through poly(vinyl alcohol) hydrogel membranes, *Biomaterials* 15 (1994) 231–238.
- [41] P.K. Smith, R.I. Krohn, G.T. Hermanson, A.K. Mallia, F.H. Gartner, M.D. Provenzano, E.K. Fujimoto, N.M. Goeke, B.J. Olson, D.C. Klenk, Measurement of protein using bicinchoninic acid, *Anal. Biochem.* 150 (1985) 237–245.
- [42] P. Shih, B.A. Malcolm, S. Rosenberg, J.F. Kirsch, A.C. Wilso, Reconstruction and testing of ancestral proteins, *Methods Enzymol.* 224 (1993) 576–590.
- [43] J. Crank, *The Mathematics of Diffusion*, Clarendon Press, Oxford, 1975.
- [44] A.W. Watkins, K.S. Anseth, Investigation of molecular transport and distributions in poly(ethylene glycol) hydrogels with confocal laser scanning microscopy, *Macromolecules* 38 (2005) 1326–1334.
- [45] S.C. De Smedt, T.K.L. Meyvis, J. Demeester, Diffusion of macromolecules in dextran methacrylate solutions and gels as studied by confocal scanning laser microscopy, *Macromolecules* 30 (1997) 4863–4870.
- [46] T.K.L. Meyvis, S.C. De Smedt, P. Van Oostveldt, J. Demeester, Fluorescence recovery after photobleaching: a versatile tool for mobility and interaction measurements in pharmaceutical research, *Pharm. Res.* 16 (8) (1999) 1153–1162.
- [47] K. Braeckmans, L. Peeters, N.N. Sanders, S.C. De Smedt, J. Demeester, Three-dimensional fluorescence recovery after photobleaching with the confocal scanning laser microscope, *Biophys. J.* 85 (2003) 2240–2252.
- [48] S.B. Petersen, V. Jonson, P. Fojan, R. Wimmer, S. Pedersen, Sorbitol prevents the self-aggregation of unfolded lysozyme leading to an up to 13 °C stabilisation of the folded form, *J. Biotechnol.* 114 (3) (2004) 269–278.
- [49] J. Hu, S. Li, B. Liu, Adsorption of BSA onto sulfonated microspheres, *Biochem. Eng. J.* 23 (3) (2005) 259–263.
- [50] M. van de Weert, W.E. Hennink, W. Jiskoot, Protein instability in poly(lactic-co-glycolic acid) microparticles, *Pharm. Res.* 17 (10) (2000) 1159–1167.
- [51] S.P. Schwendeman, Recent advances in the stabilization of proteins encapsulated in injectable PLGA delivery systems, *Crit. Rev. Ther. Drug Carr. Syst.* 19 (1) (2002) 73–98.
- [52] W. Jiang, R.K. Gupta, M.C. Deshpande, S.P. Schwendeman, Biodegradable poly(lactic-co-glycolic acid) microparticles for injectable delivery of vaccine antigens, *Adv. Drug Deliv. Rev.* 57 (3) (2005) 391–410.
- [53] H. Tamber, P. Johansen, H.P. Merkle, B. Gander, Formulation aspects of biodegradable polymeric microspheres for antigen delivery, *Adv. Drug Deliv. Rev.* 57 (3) (2005) 357–376.
- [54] L. Li, S.P. Schwendeman, Mapping neutral microclimate pH in PLGA microspheres, *J. Control. Release* 101 (2005) 163–173.
- [55] A. Lucke, J. Kiermaier, A. Göpferich, Peptide acylation by poly(alpha-hydroxy esters), *Pharm. Res.* 19 (2) (2002) 175–181.
- [56] W.E. Hennink, H. Talsma, J.C.H. Borchert, S.C. De Smedt, J. Demeester, Controlled release of proteins from dextran hydrogels, *J. Control. Release* 39 (1996) 47–55.